Coadsorption Studies of Tris(1,10-phenanthroline)ruthenium(II) and *N*-Methylated Alkaloid Cation by Laponite with an Application for a Chiral Column Packing Material

Norishige Kakegawa and Akihiko Yamagishi*,†

Department of Earth and Planetary Science, Graduate School of Science, University of Tokyo, 113-0033, Bunkyo-ku Hongo 7-3-1, Tokyo, Japan

Received September 30, 2004. Revised Manuscript Received January 13, 2005

Coadsorption studies of chiral tris(1,10-phenanthroline)ruthenium(II) ($[Ru(phen)_3]^{2+}$) and *N*-methylated cinchona alkaloid cation (MQN^+) were conducted on a smectite clay by ion exchange reactions. Photoinduced energy transfer between these cations was confirmed by the photoluminescence spectra, indicating that the cations were co-intercalated in the interlayer space of a smectite. When a ternary ion-exchanged adduct of $[Ru(phen)_3]^{2+}/MQN^+$/smectite was employed as a packing material for liquid chromatography, the column proved to resolve a racemic mixture of 1,1′-binaphthol more effectively than the column packed with a binary adduct of $[Ru(phen)_3]^{2+}$/smectite. The results reflected the enhancement of the chiral discrimination ability through the cooperative interactions among two kinds of preadsorbed chiral cations.

Introduction

A smectite group of layered clay minerals has been applied in a wide range of scientific research due to their unique properties such as two-dimensional expandable interlayer space, large surface area, cation exchange ability, and remarkable stability against chemical and physical destruction.[1−4] As one of these characteristics, a smectite can accommodate various organic cations into its interlayer space. The resultant organically modified smectites are used as adsorbents for nonionic organic compounds,[2,5−6] since the combination of hosts and guests for wide ranges of layer charge density (host) and molecular geometry (guest) leads to the controlled adsorptive properties of organically modified smectites.

Along this line, organically modified smectites have been applied as a packing material for liquid column chromatography due to their selective adsorptive properties.[7−9] In particular, the intercalation of chiral metal complexes such as tris(2,2′-bipyridine)ruthenium(II) (abbreviated as $[Ru(bpy)_3]^{2+}$) and tris(1,10-phenanthroline)ruthenium(II) (abbreviated as $[Ru(phen)_3]^{2+}$) by a smectite has been studied to understand the nature of the host−guest systems[10,11] as well as to construct an adsorbent,[12] optical resolving agent,[13] and a chiral catalysis.[14] The method of optical resolution by use of a chiral metal complex−clay intercalation compounds was based on the chiral discrimination through the intermolecular interactions between an adsorbed metal complex and a resolved molecule.

One possibility to improve selectivity toward a wider range of racemic compounds is to coadsorb two different kinds of chiral cationic molecules on a smectite. The cooperative interactions of adsorbed cations might exhibit higher selectivity than either one of the adsorbates alone does. The intercalation of two cationic species, however, often results in segregation, where they are intercalated in the different gallery spaces.[15] Hence, the proper combination of two kinds of the preadsorbed chiral cationic molecules is most important in order to construct a clay−organic intercalation compound with optimum molecular discrimination.

* To whom correspondence should be addressed. E-mail: yamagisi@eps.s.u-tokyo.ac.jp.

† Also at: CREST, Japan Science and Technology Agency.

(1) Ogawa, M.; Kuroda, K. *Chem. Rev.* **1995**, *95*, 399.
(2) Ogawa, M.; Kuroda, K. *Bull. Chem. Soc. Jpn.* **1997**, *70*, 2593.
(3) Theng, B. K. G. *The Chemistry of Clay-Organic Reactions*; Adam Hilger: London, 1974.
(4) Van Olphen, H. *An Introduction to Clay Colloid Chemistry*, 2nd ed.; Wiley-Interscience: New York, 1977.
(5) Barrer, R. M. *Zeolites and Clay Minerals as Sorbents and Molecular Sieves*; Academic Press: London, 1978.
(6) Barrer, R. M. *Clays Clay Miner.* **1989**, *37*, 385.
(7) Mingelgrin, U.; Tsvetkow, F. *Clays Clay Miner.* **1985**, *33*, 285.
(8) Tsvetkow, F.; Mingelgrin, U. *Clays Clay Miner.* **1987**, *35*, 391.
(9) Tsvetkow, F.; Mingelgrin, U.; Lahav, N. *Clays Clay Miner.* **1990**, *38*, 380.
(10) (a) Joshi, V.; Kotkar, D.; Ghosh, P. K. *Curr. Sci.* **1988**, *57*, 567. (b) Joshi, V.; Ghosh, P. K. *J. Am. Chem. Soc.* **1989**, *111*, 5604. (c) Kamat, P. V.; Gopidas, K. R.; Mukherjee, T.; Joshi, V.; Kotkar, D.; Pathak, V. S.; Ghosh, P. K. *J. Phys. Chem.* **1991**, *95*, 10009. (d) Taniguchi, M.; Kaneyoshi, M.; Nakamura, Y.; Yamagishi, A.; Iwamoto, T. *J. Phys. Chem.* **1990**, *94*, 5896. (e) Taniguchi, M.; Yamagishi, A.; Iwamoto, T. *Inorg. Chem.* **1991**, *30*, 2462. (f) Yamagishi, A. *Inorg. Chem.* **1985**, *24*, 1689.
(11) (a) Sato, H.; Yamagishi, A.; Kato, S. *J. Am. Chem. Soc.* **1992**, *114*, 10933. (b) Sato, H.; Yamagishi, A.; Kato, S. *J. Phys. Chem.* **1992**, *96*, 9377. (c) Sato, H.; Yamagishi, A.; Kato, S. *J. Phys. Chem.* **1992**, *96*, 9382. (d) Sato, H.; Yamagishi, A.; Naka, K.; Kato, S. *J. Phys. Chem.* **1996**, *100*, 1711.
(12) Okada, T.; Morita, T.; Ogawa, M. *Appl. Clay Sci.*, in press.
(13) (a) Yamagishi, A. *J. Chromatogr.* **1983**, *262*, 41. (b) Yamagishi, A. *J. Chem. Soc., Chem. Commun.* **1983**, 9. (c) Yamagishi, A. *J. Chromatogr.* **1985**, *319*, 299. (d) Yamagishi, A. *J. Am. Chem. Soc.* **1985**, *107*, 732. (e) Yamagishi, A.; Makino, H.; Nakamura, Y.; Sato, H. *Clay Clay Miner.* **1992**, *40*, 359. (f) Yamagishi, A.; Taniguchi, M.; Imamura, Y.; Sato, H. *Appl. Clay Sci.* **1996**, *11*, 1. (g) Nakamura, Y.; Yamagishi, A.; Matumoto, S.; Tohkubo, K.; Ohtu, Y.; Yamaguchi, M. *J. Chromatogr.* **1989**, *482*, 165.
(14) (a) He, J. X.; Sato, H.; Yang, P. J.; Yamagishi, A. *J. Electroanal. Chem.* **2003**, *560*, 169. (b) Hikita, T.; Tamaru, K.; Yamagishi, A.; Iwamoto, T. *Inorg. Chem.* **1989**, *28*, 2221.
(15) Ghosh, P. K.; Bard, A. J. *J. Phys. Chem.* **1984**, *88*, 5519.

10.1021/cm048285s CCC: $30.25
Published on Web 04/30/2005

Chart 1. Molecular Structure of Cinchona Alkaloid Derivative Cation Used in This Study (MQN^+)

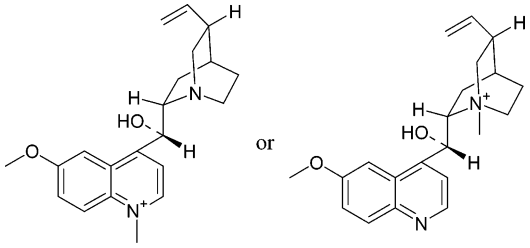

In this work, the coadsorption of chiral $[Ru(phen)_3]^{2+}$ complex and cinchona alkaloid derivative cation (Chart 1) on a smectite has been studied. Cinchona alkaloid derivatives were selected as a coadsorbate because they were among the most versatile and most highly used chiral molecule shapes in enantiomeric separations and asymmetric syntheses.[16] One of the applications is the enantioselective hydrogenation of ethyl pyruvate by using the clay−alkaloid compounds loading platinum particles.[17] Interactions among the coadsorbed chiral cations on a smectite were attempted to attain the optimum selectivity of a target racemic compound such as tris(acetylacetonato)ruthenium complex (Chart 2a) and 1,1′-binaphthol (Chart 2b).

Experimental Section

Materials. Synthetic sodium hectorite (Laponite XLG, Rockwood Additives Ltd., abbreviated as Laponite) was used after spray-drying.[18] The obtained spray-dried Laponite is the aggregate, which consists of disk-shaped Laponite particles (<0.02 μm). Each particle was spherically shaped with an average diameter of 12 μm. The elemental composition of the Laponite was stated to be $(Na_{0.70})^{+0.70}$-$Si_{8.00}(Mg_{3.50}Li_{0.30})O_{20}(OH)_4^{-0.70}$ with a cation exchange capacity (CEC) of 63 mequiv/(100 g of clay). Optically active $[Ru(phen)_3]^{2+}$ diperchlorate (abbreviated as $[Ru(phen)_3](ClO_4)_2$) was prepared as described previously.[18] *N*-Methylated quinine perchlorate (abbreviated as $MQN(ClO_4)$) was prepared as follow: 3.21 g (9.9 mmol) of quinine and 1.89 g (13.3 mmol) of iodomethane were refluxed at 353 K in benzene for 4 h under N_2 atmosphere. The precipitate was dissolved in water, and sodium perchlorate was added in the aqueous solution. The precipitate was purified by recrystallization from methanol. The ^1H NMR measurements confirmed that two kinds of MQN^+ were synthesized (Chart 1). In the present study, these MQN^+s were used as a mixture. Tris(acetylacetonato)-ruthenium(III) (Aldrich, abbreviated as $[Ru(acac)_3]$) and 1,1′-binaphthol (Kanto Kagaku Chemical, Japan) were used as received.

Table 1. Abbreviated Designation of the Products

product name	amt of added guest cations (mequiv/(100 g of clay)) Λ-,Δ-$[Ru(phen)_3]^{2+}$	MQN^+	abbreviation
Δ-$[Ru(phen)_3]^{2+}$/MQN^+−Laponite	20	0	Δ20/0-Laponite
	20	10	Δ20/10-Laponite
	20	20	Δ20/20-Laponite
	20	30	Δ20/30-Laponite
	20	40	Δ20/40-Laponite
Λ-$[Ru(phen)_3]^{2+}$/MQN^+−Laponite	20	40	Λ20/40-Laponite
MQN^+−Laponite	0	40	0/40-Laponite
	0	60	0/60-Laponite

Synthesis of $[Ru(phen)_3]^{2+}$/MQN^+−Laponite Intercalation Compounds. A 2.0 g amount of Laponite was dispersed in 100 mL of methanol and stirred for 10 min. A 50 mL aliquot of Δ-(or Λ-)$[Ru(phen)_3](ClO_4)_2$ methanol solution (11.5 mM) was added in the suspension and stirred for 4 h. Thereafter a $MQN(ClO_4)$ methanol solution was added to the suspension and stirred for 4 h. The suspension was centrifuged at 3000 rpm for 10 min. The added amount of each guest is summarized in Table 1 with the abbreviation of the products.

Preparation of Columns for Optical Resolution. The obtained intercalation compounds were dispersed in methanol in order to prepare a slurry. The slurry was packed in a 5.0 0.4 cm stainless tube using a slurry packer (SC-30, JASCO Ltd.). A 200 mL aliquot of methanol was flowed in the stainless tube in 4 h to pack the slurry.

Characterization. The X-ray powder diffraction patterns of the products were recorded on a Rigaku Rint Ultima System using monochromatic Cu Kα radiation. The UV−vis absorption spectra of the $[Ru(phen)_3]^{2+}$/MQN^+−Laponite methanol suspensions were recorded on a Hitachi U-2810 spectrophotometer. The photoluminescence spectra of the $[Ru(phen)_3]^{2+}$/MQN^+−Laponite methanol suspensions were recorded on a FP 6500 specrofluorometer (JASCO Ltd.). Luminescence lifetimes were measured by a single-photon-counting technique on a HORIBA NAES-700 time-correlated spectrophotometer equipped with a hydrogen lamp. These measurements were conducted under ambient atmosphere at room temperature. Since $[Ru(phen)_3]^{2+}$/MQN^+−Laponite did not swell in methanol, the suspensions were stirred during the UV−vis, photoluminescence, and luminescence lifetime measurements. The absolute configuration of each enantiomer was determined from the circular dichroism spectra with a polarimeter J-700 (JEOL). The chromatogram was recorded with a UV-975 (JASCO Ltd.). About 1000 ppm of either a racemic mixture or an enantiomer of $[Ru(acac)_3]$ and 1,1′-binaphthol was mounted and eluted with methanol. The elution was monitored by absorbance at 400 and 345 nm for $[Ru(acac)_3]$ and 1,1′-binaphthol, respectively. The dead volume of a column was obtained by injecting 5 μL of chloroform, assuming that chloroform was not adsorbed by the column.

Results and Discussions

Intercalation of $[Ru(phen)_3]^{2+}$ and MQN^+ into the Interlayer Space of Laponite. By the reactions of Laponite with $[Ru(phen)_3]^{2+}$ and MQN^+, orange solids were obtained. The quantitative adsorption of the added cationic guests was confirmed by the UV−vis absorption spectra of a supernatant where the metal-to-ligand charge transition (MLCT) band of $[Ru(phen)_3]^{2+}$ (around 450 nm) and the $\pi-\pi^*$ band of MQN^+ (around 325 nm) were measured as a characteristic peak. The XRD patterns of Laponite and the orange products prepared by the reaction with Laponite and cationic guests

(16) (a) Jacobsen, E. N.; Marko, I.; Mungall, W. S.; Schrader, G.; Sharpless, K. B. *J. Am. Chem. Soc.* **1988**, *110*, 1968. (b) Wai, J. S. M.; Marko, I.; Svendsen, J. S.; Finn, M. G.; Jacobsen, E. N.; Sharpless, K. B. *J. Am. Chem. Soc.* **1989**, *111*, 1123. (c) Amberg, W.; Bennani, Y. L.; Chadha, R. K.; Crispino, G.A.; Davis, W. D.; Hartung, J.; Jeong, K.-S.; Ogino, Y.; Shibata, T.; Sharpless, K. B. *J. Org. Chem.* **1993**, *58*, 844. (d) O'Donnel, M. J.; Bennett, W. D.; Wu, S. *J. Am. Chem. Soc.* **1989**, *111*, 2353. (e) Kumar, A.; Salunkhe, R. V.; Rane, R. A.; Dike, S. Y. *J. Chem. Soc., Chem. Commun.* **1991**, 485. **(f)** Wynberg, H. *Top. Stereochem.* **1986**, *16*, 87. (g) Puzicha, G.; Lightner, D. A. *J. Am. Chem. Soc.* **1991**, *113*, 3583. (h) Rosini, C.; Altemura, P.; Phi, D.; Bertucci, C.; Zullino, G.; Salvadori, P. *J. Chromatogr.* **1985**, *348*, 79. (i) Miyoshi, K.; Nataubori, M.; Dohmoto, N.; Izumoto, S.; Yoneda, H. *Bull. Chem. Soc. Jpn.* **1985**, *58*, 1529. (j) Salvadori, P.; Pini, D.; Rosini, C.; Bertucci, C. *Chirality* **1992**, *4*, 43.
(17) Mastalir, A.; Szollosi, G.; Kiraly, Z.; Razga, Z. *Appl. Clay Sci.* **2002**, *22*, 9.
(18) Tokubo, K.; Yamaguchi, M.; Ohtsu, Y.; Nakamura, K.; Matsumoto, S.; Yamagishi, A. Eur. Pat. Appl., 1989, 17 pp. CODEN: EPXXDW EP 297901 A1 19890104 CAN 111:32857 AN 1989:432857 CAPLUS.
(19) Gillard, R. D.; Hill, R. E. E. *J. Chem. Soc., Dalton Trans.* **1974**, 1217.

Chart 2. Molecular Structure of the Tris(acetylacetonato)ruthenium Complex ([Ru(acac)$_3$], a) and 1,1′-Binaphthol (b)

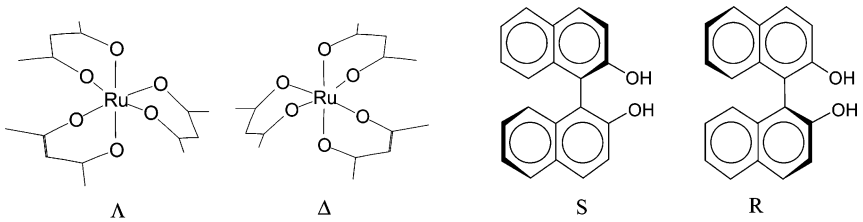

(a) (b)

are shown in Figure 1. The loading amounts and compositions of cationic guests are denoted by a notation, Δ*x*/*y*-Laponite, in which Δ*x* and *y* denote the amounts of Δ-$[Ru(phen)_3]^{2+}$ and MQN^+ adsorbed by Laponite in terms of milliequivalents per 100 g of clay, respectively. The basal spacing of the products (1.52, 1.72, 1.72, and 1.81 nm for Δ20/0-, 0/40-, 0/60-, and Δ20/40-Laponite, respectively) was longer than that of the Laponite (Figure 1a, 1.23 nm), confirming the adsorption of the cationic guests in the interlayer space of Laponite. The heights of $[Ru(phen)_3]^{2+}$ along its C_3 axis and a MQN^+ molecule are both estimated to be ca. 0.80 nm. Subtracting the thickness of the silicate layer (0.96 nm) from the basal spacing, the height of the gallery space is estimated to be 0.56 nm for the Δ20/0-Laponite (1.52 nm). This value is smaller than the height of $[Ru(phen)_3]^{2+}$, suggesting that the diffraction peak shown in the XRD pattern of the Δ20/0-Laponite consists of two peaks and the ion segregation between the adsorbed $[Ru(phen)_3]^{2+}$ and sodium cation was confirmed. On the other hand, the basal spacing of the Δ20/40-Laponite (1.81 nm) was large compared with the basal spacing of 0/40- and 0/60-Laponite (1.72 nm). These results suggested that the addition of MQN^+ led to the uniform expansion of the basal spacing of the $[Ru(phen)_3]^{2+}$−Laponite. Based on this, $[Ru(phen)_3]^{2+}$ and MQN^+ were concluded to intercalate in the same interlayer space of Laponite. The gallery height of the $[Ru(phen)_3]^{2+}$/MQN^+−Laponite was calculated to be 0.85 nm from the basal spacing (1.81 nm), indicating that the guests were intercalated in the interlayer space of the Laponite as a monomolecular layer.

Figure 2 shows the effect of the loading of MQN^+ on the XRD patterns of the $[Ru(phen)_3]^{2+}$/MQN^+−Laponite at the constant loading of $[Ru(phen)_3]^{2+}$. Low MQN^+ loadings (Δ20/0- and Δ20/10-Laponte) resulted in the ion segregation. Contrarily, when the added MQN^+ amount was large (Δ20/30- and Δ20/40-Laponte), the basal spacing of the products was 1.81 nm and no other minor phases were detected. These results suggested that the adsorbed guests were intercalated without segregation, although the precise distribution of the adsorbed $[Ru(phen)_3]^{2+}$ and MQN^+ in the interlayer space of Laponite was not clear.

Fluorescence Quenching of Intercalated MQN^+ in the Interlayer Space of Laponite. The UV−vis absorption spectra of Δ20/0- and Δ20/40-Laponite methanol suspensions are shown in Figure 3. In both of the absorption spectra, the MLCT absorption band of $[Ru(phen)_3]^{2+}$ appeared around 450 nm. No spectral shift of the MLCT bands was observed by the addition of MQN^+. The absorption spectrum of a Δ20/40-Laponite methanol suspension (Figure 3b) showed the $\pi-\pi^*$ absorption band of the MQN^+ band around 334 nm. The emission spectra of the $[Ru(phen)_3]^{2+}$/MQN^+−Laponite methanol suspension under an excitation at 450 nm are

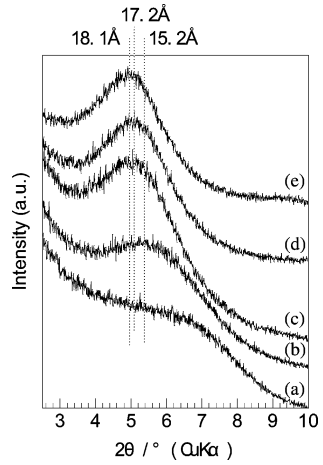

Figure 1. XRD patterns of Laponite (a), Δ20/0-Laponite (b), 0/40-Laponite (c), 0/60-Laponite (d), and Δ20/40-Laponite (e).

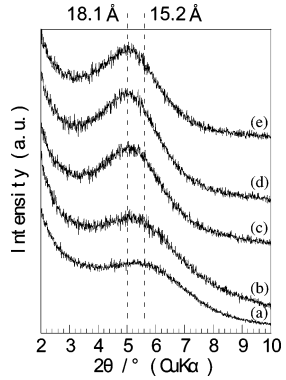

Figure 2. XRD patterns of Δ20/0-Laponite (a), Δ20/10-Laponite (b), Δ20/20-Laponite (c), Δ20/30-Laponite (d), and Δ20/40-Laponite (e).

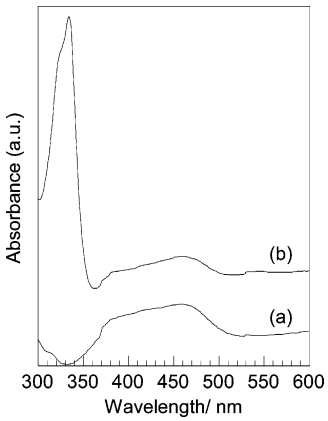

Figure 3. UV−vis absorption spectra of Δ20/0-Laponite (a) and Δ20/40-Laponite (b) methanol suspension. The concentration of the intercalation compound to methanol was 20 mg/(4 mL).

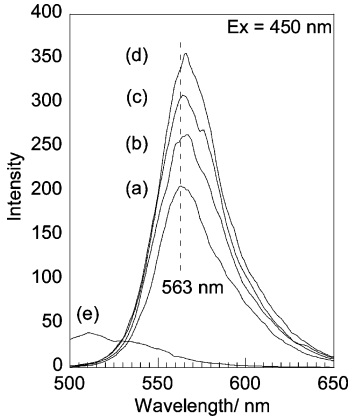

Figure 4. Emission spectra of the Δ20/0-Laponite (a), Δ20/10-Laponite (b), Δ20/20-Laponite (c), Δ20/40-Laponite (d), and 0/40-Laponite (e) methanol suspensions. The excitation wavelength was 450 nm.

shown in Figure 4. The excitation wavelength (450 nm) corresponded to the absorption band due to the adsorbed $[Ru(phen)_3]^{2+}$. Since no fluorescence due to the adsorbed MQN^+ was detected around 560 nm (Figure 4, 0/40) under this condition, the emission around 560 nm was concluded to arise exclusively from the adsorbed $[Ru(phen)_3]^{2+}$. The luminescence due to the MLCT transition of the adsorbed $[Ru(phen)_3]^{2+}$ was observed around 560 nm. Compared with the emission maximum of the $[Ru(phen)_3]^{2+}$ in methanol solution (572 nm), the luminescence of the adsorbed $[Ru(phen)_3]^{2+}$ observed around 560 nm was shifted toward a shorter wavelength region. This blue shift could be explained by the fixation of a luminescent species on a surface or rigidochromism.[20] It was hypothesized that an increased possibility for relaxation in a more fluid state caused the spectral shifts. In the present system, the intercalation of the $[Ru(phen)_3]^{2+}$ is thought to fix the $[Ru(phen)_3]^{2+}$ rigidly to cause the spectral blue shifts. The luminescence maximum stayed constant at 560 nm when the loading of Δ-$[Ru(phen)_3]^{2+}$ increased to (Δ20/0). This result indicated that the intermolecular interactions in the interlayer space of the Laponite are thought to be constant in the Δ1/0 to Δ20/0 region.

Compared with the luminescence of the adsorbed Δ-$[Ru(phen)_3]^{2+}$ on Laponite (Δ20/0, 560 nm), the luminescence maximum was slightly shifted toward the longer wavelength (ca. 3 nm) when the MQN^+ was coadsorbed on Laponite (Δ20/40, 563 nm). In the present system, both the increase of hydrophobicity of the microenvironment around the intercalated $[Ru(phen)_3]^{2+}$ by the adsorption of MQN^+ and the relaxed rigidochromism are thought as the origin of the red shift. Colón and co-workers found the concentration dependence of the luminescence maximum for $[Ru(bpy)_3]^{2+}$ intercalated in zirconium phosphate sulfophenylphosphonate at different loadings. They attributed the spectral shifts to a hydrocarbon-like environment, both by neighboring bipyridine and by the hydrophobic nature of phenyl rings.[21] Ogawa et al. reported the intercalation of $[Ru(bpy)_3]^{2+}$ into the swelling mica−poly(vinylpyrrolidone) intercalation compound.[22] The luminescence maxima of the intercalated $[Ru(bpy)_3]^{2+}$ shifted gradually toward the shorter wavelength with the decrease of the loading of $[Ru(bpy)_3]^{2+}$, reflecting the variation in the microenvironments of the intercalated $[Ru(bpy)_3]^{2+}$. In the present system, the red shift reflected the increase of hydrophobicity of the microenvironment around the intercalated $[Ru(phen)_3]^{2+}$ by the adsorption of MQN^+.

The luminescence intensity of $[Ru(phen)_3]^{2+}$ became stronger as the amount of the adsorbed MQN^+ increased. This result indicated that the self-quenching of the adsorbed $[Ru(phen)_3]^{2+}$ was suppressed as a consequence of the dilution of the surface density caused by the addition of MQN^+.

It was pointed out that the self-quenching of the excited $[Ru(bpy)_3]^{2+}$ was observed even at a low loading of the $[Ru(bpy)_3]^{2+}$ on a smectite (a few milliequivalents per 100 g of clay).[15] Ogawa et al. reported the suppression of the self-quenching of the adsorbed $[Ru(bpy)_3]^{2+}$ on a clay by the aid of poly(vinylpyrrolidone).[22,23] The hydrophilic polymer coadsorbed in the interlayer space of a swelling mica and controlled the distribution of the adsorbed $[Ru(bpy)_3]^{2+}$. Sasai et al. reported the coadsorption of rhodamine 6G and cetyltrimethylammonium cations on montmorillonite in order to construct a light-emitting material.[24] The fluorescence of rhodamine 6G could be detected at a loading as low as less than 0.5 mequiv/(100 g of clay), suggesting that alkylammonium cation has an effect of suppressing the self-quenching of the coadsorbed dye. Hagerman et al. reported that the coadsorption of the cationic surfactant and $[Ru(bpy)_3]^{2+}$ on a Laponite cast film resulted in the suppression of the luminescence self-quenching of the adsorbed $[Ru(bpy)_3]^{2+}$.[25] Compared with these reported systems, it is safely deduced that the increase of the luminescence intensity of the $[Ru(phen)_3]^{2+}$ in the present system is an indication of the coadsorption of $[Ru(phen)_3]^{2+}$ and MQN^+ on a Laponite surface.

Figure 5 shows the emission spectra of methanol suspension of the $[Ru(phen)_3]^{2+}/MQN^+$−Laponite under an excitation at 325 nm. The excitation wavelength (325 nm) corresponded to the absorption band due to the adsorbed MQN^+. In fact, the emission spectrum of the 0/40-Laponite suspension (Figure 5e) showed the fluorescence due to the adsorbed MQN^+ around 440 nm.[26,27] Notably the fluorescence of the adsorbed MQN^+ disappeared in the presence of the $[Ru(phen)_3]^{2+}$ (Figure 5a−d). Concomitantly the luminescence intensity of the adsorbed $[Ru(phen)_3]^{2+}$ increased by the addition of the MQN^+. These results indicated that the photoinduced energy transfer from the excited MQN^+

(20) Innocenzi, P.; Kozuka, H.; Yoko, T. *J. Phys. Chem. B* **1997**, *101*, 2285.
(21) Colón, J. L.; Yang, C.-Y.; Clearfield, A.; Martin, C. R. *J. Phys. Chem.* **1990**, *94*, 874.
(22) Ogawa, M.; Tsujimura, M.; Kuroda, K. *Langmuir* **2000**, *16*, 4202.
(23) Ogawa, M.; Inagaki, M.; Kodama, N.; Kuroda, K.; Kato, C. *J. Phys. Chem.* **1993**, *97*, 3819.
(24) Sasai, R.; Iyi, N.; Fujita, T. H.; Takagi, K.; Itoh, H. *Chem. Lett.* **2003**, *32*, 550.
(25) Hagerman, M. E.; Salamone, S. J.; Herbst, R. W.; Payeur, A. L. *Chem. Matter.* **2003**, *15*, 443.
(26) Shiu, F. M.; Chen, M. H.; Tang, R. F.; Jeng, Y. J.; Chang, M. Y.; Perng, J. H. *J. Non-Cryst. Solids* **1997**, *209*, 61.
(27) Rocha, C. J.; Gehlen, M. H.; da Silva, R.; Donate, P. M. *J. Photochem. Photobiol., A* **1999**, *123*, 129.

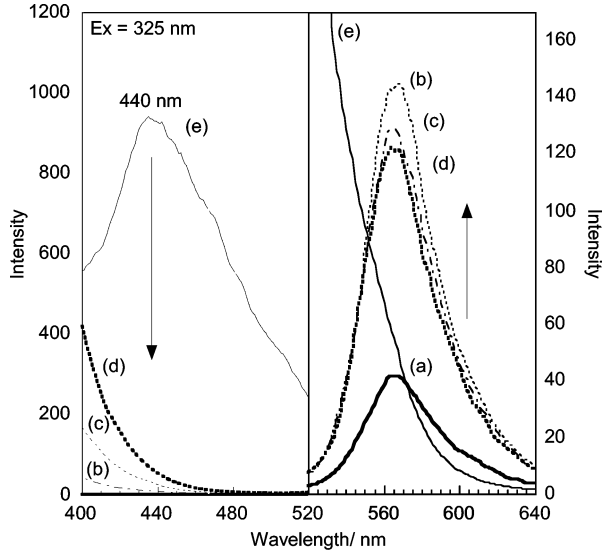

Figure 5. Emission spectra of the Δ20/0-Laponite (a), Δ20/10-Laponite (b), Δ20/20-Laponite (c), Δ20/30-Laponite (d), and Δ20/40-Laponite (e) methanol suspensions. The excitation wavelength was 325 nm.

Table 2. Luminescence Life Times of the Adsorbed Δ-$[Ru(phen)_3]^{2+}$ on Laponite

$[Ru(phen)_3]^{2+}/MQN^+$	τ_1, ns	Q_1, %	τ_2, ns	Q_2, %	χ^2
Δ20/0	1150	88	302	12	1.04
Δ20/5	1340	88	318	12	1.06
Δ20/10	1460	87	395	13	1.07
Δ20/20	1680	86	413	14	1.07
Δ20/40	1160	82	305	18	1.08

to the coadsorbed $[Ru(phen)_3]^{2+}$ took place on Laponite surfaces. The fluorescence quenching of a quinine cation by an energy acceptor such as a halide ion has been previously reported.[28] The quenching process was explained by the charge-transfer mechanism between a quinine cation and a halide ion.[28] In the present system, taking into account the overlap of the wavelength between the fluorescence of the MQN^+ (440 nm, Figure 5e) and the MLCT absorption band of the $[Ru(phen)_3]^{2+}$ (450 nm, Figure 3), the quenching mechanism of MQN^+ may be explained in terms of the Förster-type energy transfer although further experimental data are needed to confirm the quenching mechanism such as the luminescence lifetimes of the adsorbed guests. The occurrence of the effective photochemical reaction between the coadsorbed guests on Laponite, however, indicated that the $[Ru(phen)_3]^{2+}$ and MQN^+ cations were intercalated into the same interlayer space of the Laponite without segregation.

The results of the luminescence lifetime of the adsorbed $[Ru(phen)_3]^{2+}$ on Laponite are shown in Table 2. The excitation light through the band-pass filter (B390, HOYA Corp.) was used. By the light irradiation, both the adsorbed MQN^+ and Δ-$[Ru(phen)_3]^{2+}$ were excited. All the luminescence decay curves of the intercalation compounds were fitted by a double-exponential model, which is expressed as

$$I(t) = A_1 \exp(-k_1 t) + A_2 \exp(-k_2 t) \quad (1)$$

where $I(t)$ is luminescence intensity at time t, A_1, and A_2 are preexponential factors, and k_1 and k_2 are decay rate constants, respectively. The decay was fitted to a major long-lived component with a minor short-lived component. Except for the system of the Δ20/40, the luminescence lifetimes of the adsorbed Δ-$[Ru(phen)_3]^{2+}$ increased with the increase of the loading amount of MQN^+, indicating that the energy transfer from MQN^+ to Δ-$[Ru(phen)_3]^{2+}$ took place on a Laponite surface. On the contrary, the decrease of the luminescence lifetime of Δ-$[Ru(phen)_3]^{2+}$ in the Δ20/40-Lapontie system reflected that much amount of the adsorbed MQN^+ caused the cation segregation on Laponite and that the energy transfer could not occur effectively. This suggestion corresponded to the result that the emission intensity of the Δ-$[Ru(phen)_3]^{2+}$ in the Δ20/40 system (Figure 5d) was weaker than that of the Δ20/10 system (Figure 5b).

It has been pointed out that the intercalation of two cationic species often results in segregation, where they are intercalated in the different gallery spaces.[15] There are few examples to overcome the segregation problem to realize intermolecular reactions on smectites. For example, two cationic porphyrins (zinc and free base) were intercalated in the same interlayer space of the smectite to lead to photoinduced energy transfer.[29] Coadsorption of cationic (methyl green) and neutral (bioresmethrin) species on a smectite led to effective photoinduced energy transfer.[30] The adsorption of poly(vinylpyrrolidone) on a clay was found to assist the coadsorption of $[Ru(bpy)_3]^{2+}$ and methyl viologen dications and the photoinduced electron-transfer quenching between them.[31] The energy transfer from MQN^+ to $[Ru(phen)_3]^{2+}$ in the interlayer space of Laponite as observed here may be of great value as one of the examples to accomplish the controlled intermolecular reactions by organizing reactant on smectites.

Application of Ion Exchanged Adducts for Chromatographic Resolution. The present finding of the coadsorption of two different kinds of chiral cations by Laponite was utilized to develop a column material with higher selectivity in optical resolution. As a resolved racemic mixture, $[Ru(acac)_3]$ and 1,1′-binaphthol were employed. These molecules were known to be resolved on a column packed with an adduct of $[Ru(phen)_3]^{2+}$−Laponite. Thus, any change of the resolution ability was thought to be the effect of an added cation (MQN^+) on the resolution processes.

Figure 6 shows the chromatograms of $[Ru(acac)_3]$ when it was eluted with methanol on a column packed with $[Ru(phen)_3]^{2+}/MQN^+$−Laponite at room temperature. Except for the 0/40-Laponite column, the chromatograms consisted of two peaks, indicating the achievement of optical resolution. The capacity ratio (k') and the selectivity (α) of $[Ru(acac)_3]$ and binaphthol are presented in Table 3. Here the parameters, k' and α, are defined as

$$k'_R = (t_R - t_0)/t_0 \quad (2)$$

$$\alpha = k'_2/k'_1 \quad (3)$$

where t_R is the retention time of $[Ru(acac)_3]$ and t_0 the retention time of chloroform, assuming that chloroform was

(28) Bigger, S. W.; Watkins, P. J.; Verity, B. *Int. J. Chem. Kinet.* **2000**, *32*, 473.
(29) Takagi, S.; Tryk, D. A.; Inoue, H. *J. Phys. Chem. B* **2002**, *106*, 5455.
(30) Margulies, L.; Rozen, H.; Cohen, E. *Nature* **1985**, *315*, 658.
(31) Kakegawa, N.; Ogawa, M. *Langmuir* **2004**, *20*, 7004.

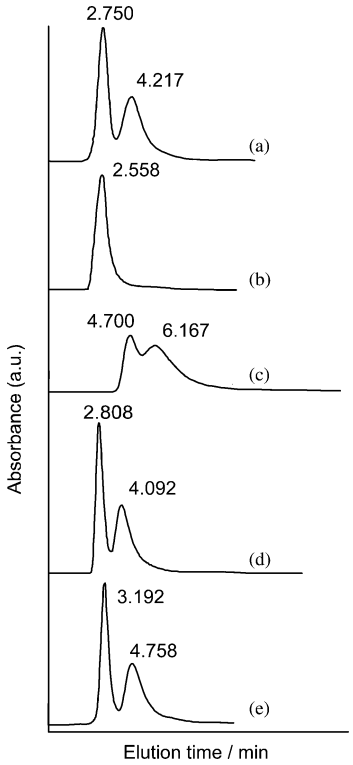

Figure 6. Chromatograms when a racemic mixture of $[Ru(acac)_3]$ was eluted with methanol on columns packed with the $[Ru(phen)_3]^{2+}/MQN^{+}-$Laponite. The packed materials were Δ20/0 (a), 0/40 (b), Δ20/40(d), and Λ20/40(e), and the column connected the columns packed with the Δ20/0- and 0/40-Laponite (c). The flow rate was 0.5 mL min^{-1}, and the elution was monitored by the absorbance at 400 nm at room temperature.

Table 3. Capacity Ratio (k'_x) and Selectivity (α) of $[Ru(acac)_3]$ and Binaphthol

	racemic compound					
	$[Ru(acac)_3]$			binaphthol		
column name	k'_1	k'_2	α	k'_1	k'_2	α
Δ20/0-Laponite	Λ,2.75	4.22	1.89	*S*,1.22	1.23	1.14
0/40-Laponite	Λ,2.40	2.68	1.21	*R*,3.36	3.68	1.14
Δ20/0-Laponite + 0/40-Laponite	Λ,4.70	6.17	1.60	*R*,4.51	4.67	1.07
Δ20/40-Laponite	Λ,2.81	4.09	1.75	*R*,2.95	3.31	1.19
Λ20/40-Laponite	Δ,3.19	4.76	1.75	*R*,3.18	3.79	1.29

not adsorbed by the column. The quantities, k'_1 and k'_2, are the capacity ratios of the enantiomers of $[Ru(acac)_3]$. The retention times, which were obtained with the chromatograms of each enantiomer, were used to calculate the k'_R in order to obtain the retention times exactly. The retention time of k'_1 is shorter than the time of k'_2. Δ or Λ in Table 3 denotes the absolute configuration of the less retained enantiomer. By using the Δ20/0- and 0/40-Laponite columns for optical resolution of $[Ru(acac)_3]$, the less retained enantiomer was found to be Λ-$[Ru(acac)_3]$. The difference of the α values of $[Ru(acac)_3]$ by using the Δ20/0-Laponite (1.89) and 0/40-Laponite (1.21) columns suggested that the stereoselective interactions between preadsorbed $[Ru(phen)_3]^{2+}$ and $[Ru(acac)_3]$ were stronger than the interactions between MQN^{+} and $[Ru(acac)_3]$. Therefore, stereoselective interactions between $[Ru(phen)_3]^{2+}$ and $[Ru(acac)_3]$ dominated when the Δ20/40-Laponite and Λ20/40-Laponite columns were used.

The cooperative effect of two kinds of cations was examined by comparing the resolution behavior between two columns: one was the Δ20/0-Laponite and 0/40-Laponite columns connected in series (column 1) and the other the Δ20/40-Laponite column (column 2). For the case of $[Ru(acac)_3]$, the α value was obtained to be 1.60 and 1.75 for columns 1 and 2, respectively. The enhancement of separation efficiency was confirmed when two cations were coadsorbed on the same Laponite. The results suggested that the ternary system among the preadsorbed $[Ru(phen)_3]^{2+}$, MQN^{+}, and the $[Ru(acac)_3]$ in the Δ20/40-Laponite column acted cooperatively in discriminating the chirality of $[Ru(acac)_3]$ on a Laponite surface. However, the α values of $[Ru(acac)_3]$ by using the Δ20/40-Laponite and Λ20/40-Laponite columns (1.75) were smaller than the value of $[Ru(acac)_3]$ by using Δ20/0-Laponite (1.89). This result suggested that the coadsorbed MQN^{+} prevented the stereoselective interactions between $[Ru(phen)_3]^{2+}$ and $[Ru(acac)_3]$.

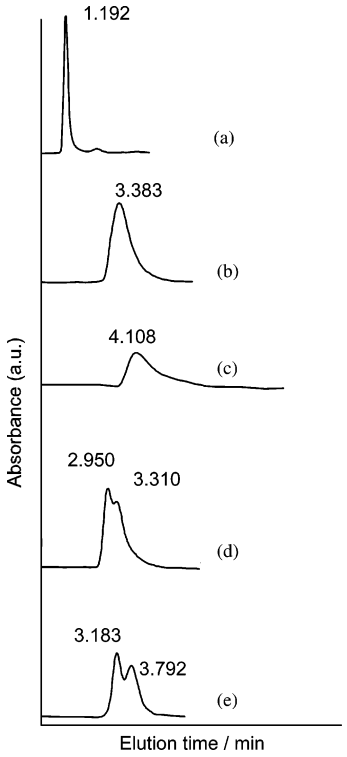

Figure 7. Chromatograms when a racemic mixture of binaphthol was eluted with methanol on columns packed with the $[Ru(phen)_3]^{2+}/MQN^{+}-$Laponite. The packed materials were Δ20/0 (a), 0/40 (b), Δ20/40(d), and Λ20/40(e), and the column connected the columns packed with the Δ20/0- and 0/40-Laponite (c). The flow rate was 0.5 mL min^{-1}, and the elution was monitored by the absorbance at 345 nm at room temperature.

Figure 7 shows the chromatograms of 1,1′-binaphthol eluted with methanol on a column packed with $[Ru(phen)_3]^{2+}/MQN^{+}-$Laponite at room temperature. Chromatograms exhibited two peaks for the cases of the Δ20/40-Laponite and Λ20/40-Laponite columns. The obtained α value was 1.19 and 1.29 for the Δ20/40-Laponite and Λ20/40-Laponite columns, respectively (Table 3). Since the values were higher than that on the Δ20/0-Laponite column, the results indicated that the effective optical resolution of binaphthol was achieved due to the cooperative interactions of the coadsorbed two cations. The difference of the α value by using the connected Δ20/40-Laponite and Λ20/40-Laponite columns reflected the stereoselectivity of each preadsorbed cation to racemic 1,1′-binaphthol.

The resolution (R_s) of 1,1′-binaphthol is expressed as

$$R_s = 1.18(t_2 - t_1)/(w_1 + w_2) \quad (4)$$

$$t_2 > t_1$$

where t_2 and t_1 are the retention times of *S*-(or *R*-)1,1′-binaphthol, and w_1 and w_2 the half-widths of the peaks. The R_s of 1,1′-binaphthol by using the Δ20/40-Laponite, Λ20/40-Laponite, and the column connected to Δ20/0- and 0/40-Laponite columns in series were calculated to be 0.233, 0.326, and 0.052, respectively. This result indicated that the ternary system for the optical resolution of the binaphthol among the preadsorbed $[Ru(phen)_3]^{2+}$, MQN^+, and the binaphthol in the interlayer space of the Laponite could have acted effectively.

We could not explain the mechanism for the cooperative interaction completely. However, we presume that the cooperative interactions were affected by the distance between adsorbed $[Ru(phen)_3]^{2+}$ and MQN^+ on Laponite. Since MQN^+ is a monocation, twice the amount of MQN^+ could be adsorbed on Laponite compared with $[Ru(phen)_3]^{2+}$. Therefore, by the addition of MQN^+, the molecular distance on the $[Ru(phen)_3]^{2+}/MQN^+$−Laponite was closer so that the gallery space was decreased. The decrease in the gallery space caused the increase in the adsorptive activity (Figures 6 and 7). As the increase in the adsorptive activity, stereoselective interaction interactions were thought to be stronger since the narrower interlayer space resulted in the increase in the molecular interactions between the preintercalated cations and binaphthol.

In addition, the difference of the α value between the Δ20/40- and Λ20/40-Laponite systems indicated that the combination of the preadsorbed guest cations ($[Ru(phen)_3]^{2+}$ and MQN^+) affected the chiral discrimination of the intercalation compounds toward the target molecules. Therefore, it was thought that the two kinds of the preadsorbed cations were related to the chiral discrimination of one chiral molecule directly. To confirm the above suggestion, further studies on understanding the distribution of the preadsorbed $[Ru(phen)_3]^{2+}$ and MQN^+ on the Laponite surface are desired.

The above chromatographic results are thought to demonstrate that the chiral discrimination ability through the intermolecular interactions among the preadsorbed guests and the target compound in the ternary system on the smectite can be controlled by the combinations of the preadsorbed guests and the racemic compound. Therefore, the studies of the organization of two kinds of preadsorbed chiral cationic molecules on a smectite are worthy of investigation in order to attain optimum selectivity toward a target racemic compound.

Conclusions

Coadsorption studies of chiral tris(1,10-phenanthroline)-ruthenium(II) ($[Ru(phen)_3]^{2+}$) and *N*-methylated cinchonia alkaloid cation (MQN^+) were conducted on a smectite clay. By the photoinduced energy transfer from the adsorbed MQN^+ to the $[Ru(phen)_3]^{2+}$, the Δ- (or Λ-)$[Ru(phen)_3]^{2+}$ and MQN^+ were concluded to be co-intercalated in the interlayer space of Laponite. The Δ- (or Λ-)$[Ru(phen)_3]^{2+}/MQN^+$−Laponite column resolved a racemic mixture of 1,1′-binaphthol to the *S*- and *R*-enantiomers effectively, indicating that chiral discrimination ability through the intermolecular interactions among the preadsorbed $[Ru(phen)_3]^{2+}$ and MQN^+ and 1,1′-binaphthol in the ternary system on a smectite realized the effective optical resolution of 1,1′-binaphthol.

Acknowledgment. This work has been financially support d by Grants-in-Aid for Scientific Research on Priority Areas (417) and No. 15340184 from the Ministry of Education, Culture, Sports, Science and Technology (MEXT) of the Japanese Government. The authors would like to thank M. Ogawa of Waseda University for using the HORIBA NAES-700 time-correlated spectrophotometer.

CM048285S